J. Biochem. **134**, 903–909 (2003)
DOI: 10.1093/jb/mvg217

Formation of Superoxide Anion during Ferrous Ion–Induced Decomposition of Linoleic Acid Hydroperoxide under Aerobic Conditions

Yasuhiro Kambayashi[*,1,2], Shozo Tero-Kubota[3], Yorihiro Yamamoto[4], Masashi Kato[2], Minoru Nakano[1], Kunio Yagi[5] and Keiki Ogino[2]

[1]Department of Photon and Free Radical Research, Japan Immunoresearch Laboratories, 351-1 Nishiyokote-cho, Takasaki 370-0021; [2]Department of Environmental and Preventive Medicine, Graduate School of Medical Science, Kanazawa University, 13-1 Takara-machi, Kanazawa 920-8640; [3]Institute of Multidisciplinary Research for Advanced Materials, Tohoku University, Sendai 980-8577; [4]School of Bionics, Tokyo University of Technology, 1404-1 Katakura, Hachioji, Tokyo 192-0982; and [5]Institute of Applied Biochemistry, Yagi Memorial Park, Mitake, Gifu 505-0116

Received May 7, 2003; accepted October 22, 2003

We studied the mechanism of formation of oxygen radicals during ferrous ion-induced decomposition of linoleic acid hydroperoxide using the spin trapping and chemiluminescence methods. The formation of the superoxide anion ($O_2^{\cdot-}$) was verified in the present study. The hydroxyl radical is also generated through Fenton type decomposition of hydrogen peroxide produced on disproportionation of $O_2^{\cdot-}$. A carbon-centered radical was detected using 5-(diethoxyphosphoryl)-5-methyl-1-pyrroline *N*-oxide (DEPMPO) as a spin trap. Alkoxyl radical formation is essential for the conversion of linoleic acid hydroperoxide into the peroxyl radical by ferrous ion. It is likely that the alkoxyl radical [$R_1CH(O^{\cdot})R_2$] is converted into the hydroxylcarbon radical [$R_1C^{\cdot}(OH)R_2$] in water, and that this carbon radical reacts with oxygen to give the *α*-hydroxyperoxyl radical [$R_1R_2C(OH)OO^{\cdot}$], which decomposes into the carbocation [$R_1C^{+}(OH)R_2$] and $O_2^{\cdot-}$.

Key words: ferrous ion–induced decomposition of linoleic acid hydroperoxide, hydrogen peroxide, hydroxyl radical, linoleic acid alkoxyl radical, superoxide anion.

Abbreviations: DEPMPO, 5-(diethoxyphosphoryl)-5-methyl-1-pyrroline *N*-oxide; DEPMPO-OH, DEPMPO-hydroxyl adduct; DEPMPO-OOH, superoxide anion adduct of DEPMPO; DMPO, 5,5-dimethyl-1-pyrroline *N*-oxide; DMPO-OH, DMPO-hydroxyl adduct; DMPO-OOH, superoxide anion adduct of DMPO; ESR, electron spin resonance; HPLC, high performance liquid chromatography; HX, hypoxanthine; LA, linoleic acid; LO$^{\cdot}$, linoleic acid alkoxyl radical; LOH, linoleic acid hydroxide; LOO$^{\cdot}$, linoleic acid peroxyl radical; LOOH, linoleic acid hydroperoxide; MCLA, 2-methyl-6-(*p*-methoxyphenyl)-3,7-dihydroimidazo[1,2-*a*]pyrazin-3-one; SOD, superoxide dismutase; XOD, xanthine oxidase.

The ferrous ion (Fe^{2+})–catalyzed decomposition of unsaturated fatty acid hydroperoxides is generally accepted to occur as shown in equation 1, in which the alkoxyl type radical and hydoxyl anion are produced (*1*, *2*).

$$LOOH + Fe^{2+} \rightarrow LO^{\cdot} + OH^{-} + Fe^{3+} \quad (1)$$

Using a spin trapping technique involving 5,5-dimethyl-1-pyrroline *N*-oxide (DMPO), however, Yagi *et al.* found that Fe^{2+}-induced decomposition of linoleic acid hydroperoxide (LOOH) generates the hydroxyl radical ($^{\cdot}OH$) under aerobic conditions (*3*). They suggested that Fe^{2+} causes homolytic cleavage of the O-O bond of LOOH (Eq. 2).

$$LOOH + Fe^{2+} \rightarrow LO^{\cdot} + {}^{\cdot}OH + Fe^{2+} \quad (2)$$

However, it is unlikely that Fe^{2+} induces the homolysis of LOOH. There is a possibility that a consecutive chain reaction helps to yield $^{\cdot}OH$. Clarification of the reaction mechanism is important because the Fe^{2+}-catalyzed decomposition of unsaturated fatty acid hydroperoxides is one of the most fundamental reactions in free radical biochemistry.

Schaich and Borg (*4*) and Chamulitrat *et al.* (*5*) also reported the formation of a spin adduct, which was comparable with the DMPO-OH adduct formed during the Fe^{2+}-catalyzed decomposition of methyl linoleate hydroperoxide under aerobic conditions. However, they proposed a different mechanism from equation 1. The former claimed that the electron spin resonance (ESR) spectrum of the DMPO-lipid alkoxyl radical spin adduct was identical to that of DMPO-OH. The latter claimed that most DMPO-OH was formed through ferric ion (Fe^{3+})–catalyzed nucleophilic addition of water to DMPO (*6*), and/or by the reaction between DMPO and $^{\cdot}OH$ produced *via* the Fenton reaction (*7*). These interpretations are in conflict. In these studies, only DMPO was used as the trapping reagent. Obviously, an ESR study with only one spin trap will not establish any mechanisms. For example, DMPO-OH is formed in various ways, as mentioned below. The superoxide anion ($O_2^{\cdot-}$) adduct of DMPO (DMPO-OOH) is a relatively short-lived spin adduct and is reduced to

[*]To whom correspondence should be addressed. Tel: +81-76-265-2217, Fax: +81-76-234-4233, E-mail: kambayashi@pub.m.kanazawa-u.ac.jp

DMPO-OH within a few min (*8*). DMPO-OH is also formed through Fe^{2+}-catalayzed decomposition of DMPO-OOH (*9*). The reaction of singlet oxygen ($^1O_2$) with DMPO also gives DMPO-OH through a Fenton-like reaction (*10*, *11*). Furthermore, DMPO-OH is produced under unexpected conditions such as on the Fe^{2+}- (*12*), Fe^{3+}- (*6*), or Fe^{3+}-bleomycin complex- (*13*) catalyzed oxidation of DMPO, or the photooxidation of DMPO (*12*). This makes it difficult to determine how DMPO-OH is produced. Recently, 5-(diethoxyphosphoryl)-5-methyl-1-pyrroline *N*-oxide (DEPMPO) was developed as a new spin trap (*14*). The $O_2^{\cdot -}$ spin adduct of DEPMPO (DEPMPO-OOH) is long-lived in comparison with DMPO-OOH (*14*, *15*). Although DEPMPO-OH is observed in the presence of DEPMPO and Fe^{3+}, a carbon-centered radical is also detected (*16*), unlike in the case where DMPO-OH is produced through Fe^{3+}-catalyzed oxidation of DMPO. Therefore, DEPMPO is a useful spin trap for discriminating $^{\cdot}OH$ from $O_2^{\cdot -}$ in a solution in which the two species coexist.

The present study was undertaken to verify the oxygen radical formation mechanism during the Fe^{2+}-catalyzed decomposition of LOOH under aerobic conditions, using the ESR spin trapping technique and the 2-methyl-6-(*p*-methoxyphenyl)-3,7-dihydroimidazo[1,2-*a*]pyrazin-3-one (MCLA)–dependent chemiluminescence methods. We used DEPMPO in addition to DMPO as a spin trap in this study.

MATERIALS AND METHODS

Materials—DMPO, lipoxidase (Type 1-B), superoxide dismutase (SOD, from bovine erythrocytes), catalase (from bovine liver), and uric acid were purchased from Sigma Chemical (St. Louis, MO). DEPMPO was obtained from *OXIS* International (Portland, OR). Ferrous sulfate ($FeSO_4$) heptahydrate and ferric chloride ($FeCl_3$) hexahydrate were purchased from Wako Pure Chemical Industries (Osaka). Linoleic acid (LA) and MCLA were obtained from Tokyo Chemical Industry (Tokyo). Solvents and other reagents were of the highest grade commercially available. LA was purified by high performance liquid chromatography (HPLC) before use. 13-Hydroperoxy-9-*cis*,11-*trans*-octadecadienoic acid (linoleic acid hydroperoxide; LOOH) was prepared using LA and lipoxidase, and LOOH was reduced to alcohol (LOH) with triphenylphosphine, and then the LOOH and LOH were purified by HPLC as previously described (*17*). The concentration of LOOH was determined using a hydroperoxide-specific, isoluminol chemiluminescence assay with HPLC (HPLC-CL) (*18*). The concentrations of LOOH and LOH were also determined using an assumed molar extinction coefficient at 234 nm, 28,000 M^{-1} cm^{-1} (*19*). DMPO was purified by filtration with decolorizing activated carbon (Aldrich Chemical Company, Milwaukee, WI) immediately before use (*8*, *20*). The concentration of DMPO was determined using an assumed molar extinction coefficient at 234 nm, 7,700 M^{-1} cm^{-1} (*21*). DEPMPO was used without further purification. The concentration of DEPMPO was calculated from its molecular weight.

Spin Trapping of Free Radicals Produced during Fe^{2+}-Catalyzed Decomposition of LOOH—A reaction mixture (450 μl) containing 2.5 mM LOOH and 613 mM DMPO was prepared in 50 mM potassium phosphate buffer (pH 7.4) pretreated with CHELEX 100 (BIO-RAD Laboratories, Hercules, CA). LOOH-decomposition was initiated by the addition of $FeSO_4$ (final concentration: 100 μM) at 25°C under aerobic conditions. LA or LOH was also used instead of LOOH. If necessary, SOD (0.5 μM), catalase (50 μg/ml), ethanol (16.7%), sodium azide (1 mM), or uric acid (100 μM) was added to the reaction mixture. $FeCl_3$ and DEPMPO (20 or 40 mM) were used instead of $FeSO_4$ and DMPO, respectively. An aliquot of the reaction mixture was transferred to a flat cell and ESR signals were measured with a BRUKER ESR spectrometer (ESP 300E. Karlsruhe, Germany) at 25°C. The measurement conditions are given in each figure legend. To avoid photo-induced reactions, sample preparation and measurements were carried out under weak red light. If necessary, argon gas was introduced into a solution for 2 h under a nitrogen atmosphere in a glove box prior to the measurement. A reaction solution was transferred to a flat cell. ESR signals were measured at 25°C under atmospheric air after the flat cell had been sealed with a teflon seal under a nitrogen atmosphere.

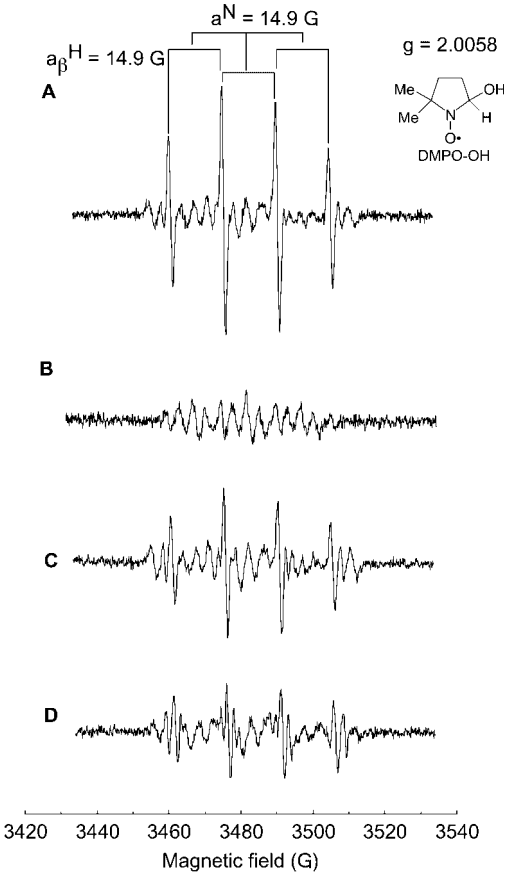

Fig. 1. **ESR spectra of the DMPO-free radical spin adducts formed during the Fe^{2+}-catalyzed decomposition of LOOH, and the effects of SOD and catalase thereon.** A: 2.2 mM LOOH + 100 μM Fe^{2+} + 613 mM DMPO, B: A – 2.2 mM LOOH, C: A + 0.5 μM SOD, D: A + 50 μg/ml catalase. Receiver gain: 2.5×10^5; modulation frequency: 100 kHz; modulation amplitude: 1.011 G; conversion: 81.920 ms; time constant: 40.960 ms; sweep time: 83.883 s; microwave frequency: 9.779 GHz; microwave power: 7.73 mW; scan number: ×10.

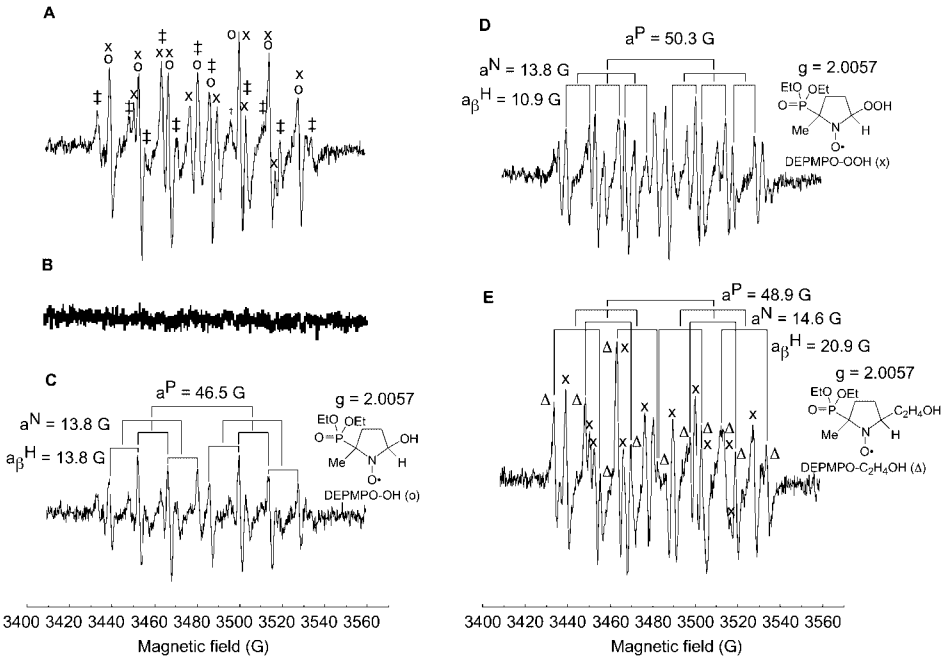

Fig. 2. **ESR spectra of the DEPMPO-free radical spin adducts formed during the Fe^{2+}-catalyzed decomposition of LOOH, and the effects of SOD, catalase, and ethanol thereon.** o, x, ‡, and Δ represent the DEPMPO-OH spin adduct, DEPMPO-OOH spin adduct, DEPMPO-carbon-centered radical adduct, and DEPMPO-hydroxyethyl spin adduct, respectively. A: 2.2 mM LOOH + 100 μM Fe^{2+} + 40 mM DEPMPO, B: A – 2.2 mM LOOH, C: A + 0.5 μM SOD, D: A + 50 μg/ml catalase, E: A + 16.7% ethanol. Receiver gain: 2.5 × 10^5; modulation frequency: 100 kHz; modulation amplitude: 1.011 G; conversion: 81.920 ms; time constant: 40.960 ms; sweep time: 83.883 s; microwave frequency: 9.779 GHz; microwave power: 23.9 mW; scan number: ×10.

Chemiluminescence during Fe^{2+}-Catalyzed Decomposition of LOOH—A reaction mixture (1 ml) comprising 50 μM LOOH and 10 μM MCLA in 50 mM potassium phosphate buffer (pH 7.4) pretreated with CHELEX 100 was placed in a luminescence reader (Type; BLR-301, Aloka, Tokyo). Chemiluminescence was detected after the addition of $FeSO_4$ (final concentration: 2 μM) at 25°C under aerobic conditions. If necessary, SOD (0.5 μM), catalase (20 μg/ml), sodium azide (1 mM), and/or DMPO (12 mM) were added to the reaction mixture. LA or LOH was also used instead of LOOH. Various concentrations of LA, LOH, LOOH, or $FeSO_4$ were also used, as described in the figure legends. If necessary, argon gas was introduced into a solution under atmospheric air for 30 min prior to the measurement. The effect of the $FeSO_4/FeCl_3$ (Fe = 2 μM) ratio on chemiluminescence intensity was also examined.

Yield of $O_2^{\cdot-}$ during Fe^{2+}-Catalyzed Decomposition of LOOH—Hypoxanthine (HX; 1 × 10^{-3} U/ml, 5 × 10^{-3} U/ml, or 1 × 10^{-3} U/ml) and xanthine oxidase (XOD; 40 μM) were incubated with cytochrome *c* (50 μM) at 25°C, the change in absorbance of cytochrome *c* at 550 nm being monitored. The amount of $O_2^{\cdot-}$ formed was calculated using the molar extinction coefficient of a reduced form of cytochrome *c* at 550 nm [21,100 M^{-1} cm^{-1} (*22*)]. The values were compared with the integrated MCLA-dependent chemiluminescence intensity obtained under the same conditions except that MCLA (10 μM) was used instead of cytochrome *c* and the amount of $O_2^{\cdot-}$ formed per chemiluminescence intensity was calculated.

Chemiluminescence intensity was measured during 2 μM Fe^{2+}-catalyzed decomposition of 36 μM LOOH with 10 μM MCLA in the presence or absence of 0.5 μM SOD at 25°C. The change in LOOH was monitored by HPLC-CL during 2 μM Fe^{2+}-induced decomposition of 36 μM LOOH, and the amount of LOOH decomposed during the present reaction was obtained. The yield of $O_2^{\cdot-}$ during Fe^{2+}-catalyzed decomposition of LOOH was calculated with the values obtained in the above experiments. [$O_2^{\cdot-}$ formed] was calculated from the SOD-sensitive MCLA-dependent chemiluminescence intensity.

$$\text{Yield of } O_2^{\cdot-}\ (\%) = [O_2^{\cdot-} \text{ formed}]\ (\mu M)/[\text{LOOH decreased}]\ (\mu M) \times 100$$

RESULTS

Spin Trapping of Free Radicals Produced during Fe^{2+}-Catalyzed Decomposition of LOOH under Aerobic Conditions—Fig. 1A shows the ESR spectrum obtained during the Fe^{2+}-induced decomposition of LOOH in the presence of DMPO. The hyperfine splitting constants of major signals were $a^N = a_\beta^H$ = 14.9 G, g = 2.0058, which were identical with those of DMPO-OH ($a^N = a_\beta^H$ = 15.0 G, g = 2.0062) (*23*). The DMPO-OH signal was not observed when LOOH was removed from the above system (Fig. 1B). The DMPO-OH signal intensity was decreased with the addition of SOD (Fig. 1C) and was substantially decreased on the addition of catalase (Fig. 1D). Chamulitrat *et al.* reported comparable results with catalase, although they used methyl linoleate hydroperoxide instead of LOOH (*5*). Separate experiments involving HPLC-CL showed that catalase (50 μg) did not decompose LOOH to the linoleic acid alkoxyl radical ($LO^{\cdot}$) or linoleic acid peroxyl radical ($LOO^{\cdot}$) (data not shown).

To obtain clearer ESR signals, we used DEPMPO as a spin trap instead of DMPO. Fig. 2A shows the ESR spectrum obtained during the Fe^{2+}-catalyzed decomposition of LOOH in the presence of DEPMPO under aerobic conditions. The ESR spectrum consists of the signals of three kinds of spin adducts: the DEPMPO-hydroxyl adduct (DEPMPO-OH) (o; a^N = 14.0 G, a_β^H = 13.0 G, a^P = 47.4 G, g = 2.0059) (*14*), the DEPMPO-OOH adduct (x; a^N = 13.4 G, a_β^H = 11.9 G, a^P = 52.5 G, g = 2.0059) (*14*), and the carbon-centered spin adduct of DEPMPO (‡; a^N = 14.5 G, a_β^H = 22.0 G, a^P = 46.0 G, g = 2.0061). The assignment of each

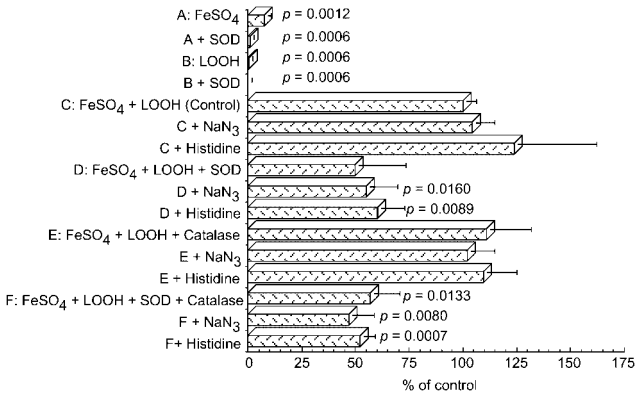

Fig. 3. **The effects of SOD (0.5 μM), catalase (20 μg/ml), sodium azide (1 mM), and/or histidine (10 mM) on the chemiluminescence observed during the 2 μM Fe^{2+}-catalyzed decomposition of 50 μM LOOH in the presence of 10 μM MCLA at 25°C under atomospheric air.** The *P* values were obtained by comparison with a control, using a paired t test.

was confirmed by means of quenching reactions with SOD, catalase and ethanol, as described below. These signals were not observed when DEPMPO was incubated with only Fe^{2+} (Fig. 2B). The addition of SOD reduced the DEPMPO-OOH signal intensity (x; Fig. 2C). The addition of catalase substantially decreased the DEPMPO-OH signal intensity (o; Fig. 2D). The addition of ethanol to the reaction mixture as an $^{\cdot}OH$ scavenger gave the ESR spectrum shown in Fig. 2E. The signals enhanced by the addition of ethanol were identified as those of the DEPMPO adduct of the hydroxyethyl radical [Δ; DEPMPO-CH(CH_3)OH] (a^N = 14.6 G, a_β^H = 21.1 G, a^P = 49.6 G, g = 2.0058; our unpublished data). The ESR parameters of DEPMPO-CH(CH_3)OH are nearly identical to those of the carbon-centered spin adduct of DEPMPO obtained in the decomposition reaction. The present spin trapping experiments suggest the generation of $O_2^{\cdot-}$, $^{\cdot}OH$, H_2O_2, and the carbon-centered radical during the Fe^{2+}-catalyzed decomposition of LOOH under aerobic conditions.

Chemiluminescence during Fe^{2+}-Catalyzed Decomposition of LOOH under Aerobic Conditions—The formation of $O_2^{\cdot-}$ during the present reaction was also examined using MCLA, which is a specific chemiluminescence probe for $O_2^{\cdot-}$ and $^1O_2$ (*24*). Fig. 3 depicts the relative intensity of MCLA-dependent chemiluminescence observed during the Fe^{2+}-catalyzed decomposition of LOOH under various conditions. The addition of SOD to the control reaction mixture significantly decreased the MCLA-dependent chemiluminescence intensity, suggesting the involvement of $O_2^{\cdot-}$ formation. Since catalase, sodium azide and histidine did not affect the chemiluminescence intensity, hydrogen peroxide (H_2O_2) and $^1O_2$

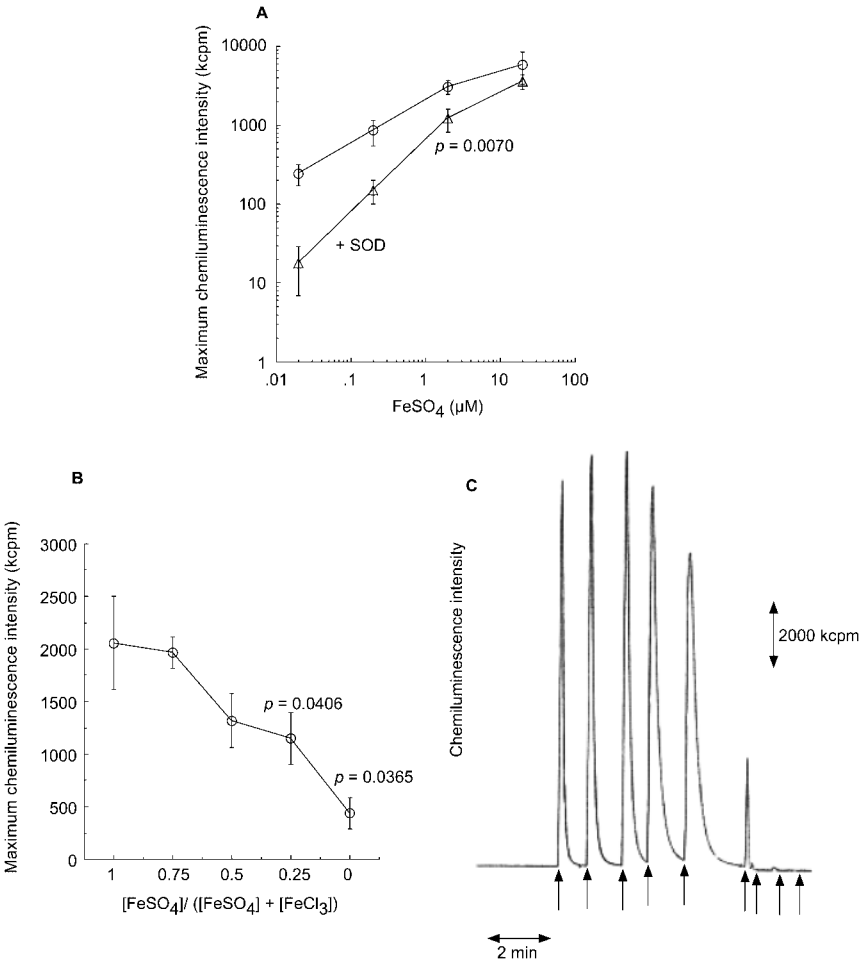

Fig. 4. **(A) The effects of the Fe^{2+} concentration on the MCLA-dependent chemiluminescence observed during the ferrous ion–catalyzed decomposition of 50 μM LOOH at 25°C in the presence (Δ) and absence (o) of SOD.** The *P* values were obtained through a paired t test, that compared the results in the presence and absence of SOD. **(B) The effect of the ratio between $FeSO_4$ and $FeCl_3$ (Fe = 2 μM) on the chemiluminescence intensity observed during the iron-catalyzed decomposition of 50 μM LOOH.** The *P* values were obtained through a paired t test involving comparison with the $FeSO_4$ (without $FeCl_3$) system. **(C) Chemiluminescence observed in the presence of 10 μM MCLA, 50 μM LOOH, and $FeSO_4$ in 50 mM potassium phosphate buffer (pH 7.4) at 25°C.** 20 μM $FeSO_4$ was added at each point indicated by an arrow.

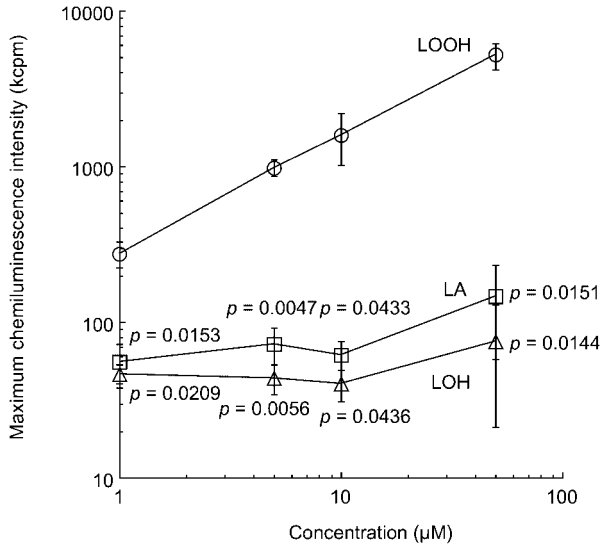

Fig. 5. **The effects of the LA, LOH and LOOH concentrations on the MCLA-dependent chemiluminescence observed during the reaction between 2 μM ferrous ion and LA, LOH, and LOOH at 25°C.** The *P* values were obtained through a paired t test involving comparison with the LOOH system.

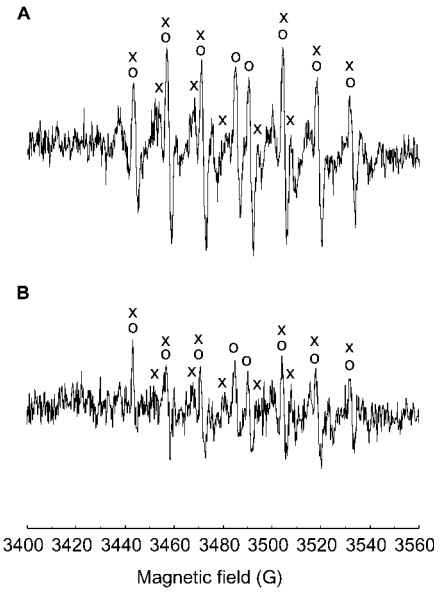

Fig. 6. **The effect of argon gas on the DEPMPO-OOH signal intensity obtained during the 100 μM ferrous ion–catalyzed decomposition of 2.2 mM LOOH in the presence of 20 mM DEPMPO at 25°C.** ESR spectra were measured at 25°C under atmospheric air. o and x represent the DEPMPO-OH spin adduct and DEPMPO-OOH spin adduct, respectively. A: No treatment, B: Argon gas bubbling. Receiver gain: 5.0×10^5; modulation frequency: 100 kHz; modulation amplitude: 2.018 G; conversion: 81.920 ms; time constant: 40.960 ms; sweep time: 83.886 s; microwave frequency: 9.779 GHz; microwave power: 9.7 mW; scan number: ×20.

were not contributors to the emission. Judging from the time-dependent change in the LOOH concentration [as monitored by HPLC-CL (*18*)], the Fe^{2+}-catalyzed decomposition of LOOH in potassium phosphate buffer stopped within an extremely short time (data not shown), probably because Fe^{2+} was chelated by phosphate and/or converted to ferric hydroxide [$Fe(OH)_3$], which is poorly soluble in water (*1*). The addition of DMPO (12 mM) had no effect on the chemiluminescence intensity (data not shown). This was due to the relatively small second-order rate constant of the reaction between $O_2^{\cdot -}$ and DMPO (10 M^{-1} s^{-1} at pH 7.8, 25°C) (*25*) in comparison with that of the reaction between MCLA and $O_2^{\cdot -}$ (2.2×10^5 M^{-1} s^{-1} at pH 7, 20°C; K. Akutsu and K. Fujimori, unpublished data).

Strong emission was not observed for the system with MCLA + Fe^{2+} or MCLA + LOOH. The chemiluminescence intensity observed during the decomposition of LOOH by Fe^{2+} was dependent on the $FeSO_4$ concentration (Fig. 4A). SOD decreased the chemiluminescence intensity but DMPO did not (data not shown). The effect of the ratio between $FeSO_4$ and $FeCl_3$ on the chemiluminescence observed during the 2 μM iron-catalyzed decomposition of LOOH was examined (Fig. 4B). When more $FeSO_4$ was in the reaction mixture, stronger chemiluminescence was observed. Moreover, the addition of 0.1–0.4 μM $FeCl_3$ to the reaction mixture containing 2 μM $FeSO_4$, 50 μM LOOH, and 10 μM MCLA had no effect on the chemiluminescence intensity (data not shown). On the other hand, chemiluminescence was observed whenever 20 μM $FeSO_4$ was added to the solution containing 10 μM MCLA and 50 μM LOOH until LOOH was completely decomposed (Fig. 4C). MCLA was not completely consumed during this experiment (data not shown). These results suggest that $FeSO_4$, not $FeCl_3$, was necessary for $O_2^{\cdot -}$ production. The intensity of the chemiluminescence was also dependent on the LOOH concentration (Fig. 5). Concentration-dependency of the chemiluminescence intensity was, however, not observed when LA or LOH was used instead of LOOH. Also, an ESR signal was not observed for the system with LA or LOH (data not shown). These results show that LOOH is necessary for the production of $O_2^{\cdot -}$ in this system, and hydroperoxide, not carboxylic group–containing compounds for chelating iron, is important for the production of $O_2^{\cdot -}$ during the Fe^{2+}-catalyzed decomposition of LOOH. Comparable but weak ESR signals and MCLA-dependent chemiluminescence were observed when Fe^{3+} was used instead of Fe^{2+} (data not shown).

Yield of $O_2^{\cdot -}$ during Fe^{2+}-Catalyzed Decomposition of LOOH—We estimated the approximate ratio of $O_2^{\cdot -}$ formed to LOOH decomposed. One count of MCLA-dependent chemiluminescence intensity corresponded to 1 fmol/ml of $O_2^{\cdot -}$ formed. The integrated MCLA-dependent chemiluminescence intensity obtained during the 2 μM Fe^{2+}-catalyzed decomposition of 36 μM LOOH was 127 ± 26 kcounts (mean ± SD, n = 3). In the presence of 0.5 μM SOD, the integrated chemiluminescence intensity was 23 ± 5 kcounts (mean ± SD, n = 3). The difference was 104 kcounts. This corresponds to 104 pmol/ml of $O_2^{\cdot -}$ formed. Since 10% of LOOH was decomposed during the reaction (data not shown), the $O_2^{\cdot -}$ formed in this system corresponded to 2.9% of LOOH decomposed.

Effect of Argon Gas in the Solvent on the Intensity of the Spin Adduct Formed during Fe^{2+}-Catalyzed Decomposition of LOOH—Figure 6 shows the effect of argon gas, introduced into the solvent, on the formation of $O_2^{\cdot -}$ during the Fe^{2+}-catalyzed decomposition of LOOH. Argon gas bubbled into each solution for 2 h under a nitrogen

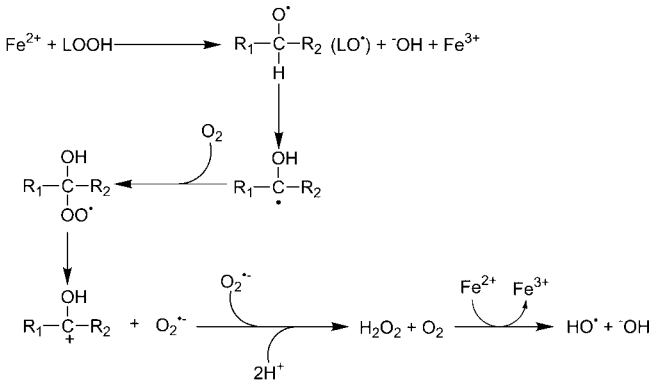

Scheme 1. **Proposed mechanism for the formation of the superoxide anion and other active oxygen species during the ferrous ion-catalyzed decomposition of linoleic acid hydroperoxide under aerobic conditions.**

atmosphere decreased the ESR signal intensities of DEPMPO adducts (DEPMPO-OOH: a_β^H = 10.7 G, a^N = 13.8 G, a^P = 50.0 G; DEPMPO-OH: a_β^H = 13.8 G, a^N = 13.6 G, a^P = 46.9 G). A weak ESR signal was observed in this case since oxygen might remain in the solution and/or the Fe^{3+}-catalyzed nucleophilic attack of water on DEPMPO might occur. The intensity of MCLA-dependent chemiluminescence observed during the Fe^{2+}-catalyzed decomposition of LOOH was also decreased to two-thirds by argon gas bubbling for 30 min under atmospheric air (data not shown).

DISCUSSION

The present study has shown that $O_2^{\cdot-}$, H_2O_2, $^{\cdot}OH$, and the carbon-centered radical are formed during the Fe^{2+}-catalyzed decomposition of LOOH under aerobic conditions. Therefore, DMPO-OH is suggested to be formed through the reaction between DMPO and $^{\cdot}OH$ produced *via* the Fenton reaction. Catalase, however, did not suppress the formation of DMPO-OH and DEPMPO-OH completely. Parts of the observed DMPO-OH and DEPMPO-OH might be produced *via* other pathways. Koga *et al.* reported (*26*) that $^1O_2$ is formed during the Fe^{3+}-catalyzed decomposition of LOOH, probably *via* the Russell mechanism (*27*). The formation of DMPO-OH during the reaction between DMPO and $^1O_2$ has also been reported (*10*, *11*). However, no effect of an $^1O_2$ quencher (sodium azide, uric acid, or histidine) on the ESR signal (data not shown) or chemiluminescence intensity was observed in the present study. Schaich and Borg reported that the spectrum of the DMPO-lipid alkoxyl radical was identical to that of DMPO-OH (*4*), but this appears not to be correct since the DMPO-linoleic acid alkoxyl radical spin adduct spectrum reported recently (*28*) was different from the DMPO-OH spectrum.

The main radical species formed during the Fe^{2+}-catalyzed decomposition of LOOH is $LO^{\cdot}$ (*1*, *2*). Therefore, MCLA may react with $LO^{\cdot}$, the MCLA radical may be formed, and light may be emitted, although MCLA is known as a specific probe for the chemiluminescent detection of $O_2^{\cdot-}$ and $^1O_2$ (*24*). Since the reaction between the MCLA radical and molecular oxygen is significantly slower than that of dimerization of the MCLA radical (*29*), MCLA does not react with oxygen to emit light in the present system. Therefore, the MCLA-dependent chemiluminescence observed in this study was caused by $O_2^{\cdot-}$.

Since each ESR spectrum was obtained by the accumulation of ten spectra obtained consecutively (each scan took 83.883 s), measurement was continued after the reaction had been stopped. On the other hand, the half-life of DMPO-OOH is 60 s (*25*) and that of DEPMPO-OOH is 890 s (*14*). Therefore, DMPO-OOH decomposed into DMPO-OH during the measurement and DEPMPO-OOH remained. For these reasons, the DEPMPO-OOH spin adduct, but not the DMPO-OOH one, might be observed during the Fe^{2+}-catalyzed decomposition of LOOH.

The present study has shown that LOOH was needed for the formation of $O_2^{\cdot-}$ during the decomposition of LOOH by Fe^{2+}. Our results also show that Fe^{2+} was needed for $O_2^{\cdot-}$ formation. The Fe^{2+}-catalyzed reduction of triplet oxygen to $O_2^{\cdot-}$ (*1*) contributed only slightly to the formation of $O_2^{\cdot-}$ in the present study (Figs. 1–3). On the other hand, introducing argon gas into the solvent reduced the intensity of both the ESR signal (Fig. 6) and the MCLA-dependent chemiluminescence (data not shown) observed during the Fe^{2+}-catalyzed decomposition of LOOH. These results suggest that oxygen dissolved in the solution, in addition to the reaction intermediate generated during the decomposition of LOOH, plays an important role in the production of $O_2^{\cdot-}$ in the present reaction system.

Recently, it was suggested that primary alkoxyl radicals (RCO^+) are converted into α-hydroxylcarbon-centered radicals through an unusual 1,2-H-atom shift in the presence of water (*30*), and the carbon-centered radicals react with dioxygen to yield α-hydroxyperoxyl radicals (*30*, *31*). It is well known that a number of peroxyl radicals decompose into carbocations and $O_2^{\cdot-}$. Therefore, we tentatively propose the mechanism of $O_2^{\cdot-}$ formation shown in Scheme 1. Conversion of $LO^{\cdot}$ $[R_1CH(O^+)R_2]$ into a hydroxycarbon-centered radical $[R_1C^+(OH)R_2]$ in water may occur, although it is a secondary alkoxyl radical. In fact, a carbon-centered radical was detected during the Fe^{2+}-catalyzed decomposition of LOOH under anaerobic conditions (*32*). In the present spin trapping experiments involving DEPMPO, the carbon-centered radical was also detected during the reaction. Then, the hydroxyperoxy radical $[R_1COO^{\cdot}(OH)R_2]$ formed through the reaction between this carbon-centered radical and molecular oxygen may decompose into a carbocation $[R_1C^+(OH)R_2]$ and $O_2^{\cdot-}$.

Finally, in this study we have demonstrated for the first time the mechanism of formation of $O_2^{\cdot-}$ (as distinct from the Fe^{2+}-catalyzed reduction of oxygen) during the Fe^{2+}-induced decomposition of LOOH under aerobic conditions.

We wish to thank Dr. Yasuhiro Kobori of Tohoku University for the advice to Y.K. regarding the ESR technique.

REFERENCES

1. Halliwell, B. and Gutteridge, J.M.C. (1999) *Free Radicals in Biology and Medicine Third Edition*, Oxford University Press, New York and Oxford
2. O'Brien, P.J. (1969) Intracellular mechanisms for the decomposition of a lipid peroxide. I. Decomposition of a lipid peroxide by metal ions, heme compounds, and nucleophiles. *Can. J. Biochem.* **47**, 485–492
3. Yagi, K., Ishida, N., Komura, S., Ohishi, N., Kusai, M., and Kohno, M. (1992) Generation of hydroxyl radical from linoleic acid hydroperoxide in the presence of epinephrine and iron. *Biochem. Biophys. Res. Commun.* **183**, 945–951
4. Schaich, K.M. and Borg, D.C. (1990) Solvent effects in the spin trapping of lipid oxyl radicals. *Free Radic. Res. Commun.* **9**, 267–278
5. Chamulitrat, W., Iwahashi, H., Kelman, D.J, and Mason, R.P. (1992) Evidence against the 1:2:2:1 quartet DMPO spectrum as the radical adduct of the lipid alkoxyl radical. *Arch. Biochem. Biophys.* **296**, 645–649
6. Makino, K., Hagiwara, T., Hagi, A., Nishi, M., and Murakami, A. (1990) Cautionary note for DMPO spin trapping in the presence of iron ion. *Biochem. Biophys. Res. Commun.* **172**, 1073–1080
7. Fenton, H.J.H. (1898) Note on the oxidation of certain acids in presence of iron. *J. Chem. Soc. Proc.* **14**, 119–120
8. Buettner, G.R. and Oberley, L.W. (1978) Considerations in the spin trapping of superoxide and hydroxyl radical in aqueous systems using 5, 5-dimethyl-1-pyrroline-1-oxide. *Biochem. Biophys. Res. Commun.* **83**, 69–74
9. Buettner, G.R. (1993) The spin trapping of superoxide and hydroxyl free radicals with DMPO (5, 5-dimethylpyrroline-N-oxide): more about iron. *Free Radic. Res. Commun.* **19 supplement**, S79–S87
10. Harbour, J.R. Issler, S.L., and Hair, M.L. (1980) Singlet oxygen and spin trapping with nitrones. *J. Amer. Chem. Soc.* **102**, 7778–7779
11. Bilski, P., Reszka, K., Bilska, M., and Chignell, C.F. (1996) Oxidation of the spin trap 5, 5-dimethyl-1-pyrroline *N*-oxide by singlet oxygen in aqueous solution. *J. Amer. Chem. Soc.* **118**, 1330–1338
12. Tero-Kubota, S., Ikegami, Y., Kurokawa, T., Sasaki, R., Sugioka, K., and Nakano, M. (1982) Generation of free radicals and initiation of radical reactions in nitrones-Fe^{2+}-phosphate buffer systems. *Biochem. Biophys. Res. Commun.* **108**, 1025–1031
13. Tero-Kubota, S., Ikegami, Y., Sugioka, K., and Nakano, M. (1987) ESR studies on the active intermediate in the enzymatic reduction of the Fe-bleomycine complex. *Biochem. Int.* **14**, 879–887
14. Frejaville, C., Karoui, H., Tuccio, B., Le Moigne, F., Culcasi, M., Pietri, S., Lauricella, R., and Tordo, P. (1995) 5-(Diethoxyphosphoryl)-5-methyl-1-pyrroline *N*-oxide: A new efficient phosphorylated nitrone for the *in vitro* and *in vivo* spin trapping of oxygen-centered radicals. *J. Med. Chem.* **38**, 258–265
15. Roubaud, V., Sankarapandi, S., Kuppusamy, P., Tordo, P., and Zweier, J.L. (1997) Quantitative measurement of superoxide generation using the spin trap 5-(diethoxyphosphoryl)-5-methyl-1-pyrroline-*N*-oxide. *Anal. Biochem.* **247**, 404–411
16. Clément, J.-L., Gilbert, B.C., Ho, W.F., Jackson, N.D., Newton, M.S., Silvester, S., Timmins, G.S., Tordo, P., and Whitwood, A.C. (1998) Use of a phosphorylated spin trap to discriminate between the hydroxyl radical and other oxidizing species. *J. Chem. Soc. Perkin Trans 2*, 1715–1717
17. Nagata, Y., Yamamoto, Y., and Niki, E. (1996) Reaction of phosphatidylcholine hydroperoxide in human plasma: The role of peroxidase and lecithin: cholesterol acyltransferase. *Arch. Biochem. Biophys.* **329**, 24–30
18. Yamamoto, Y., Brodsky, M.H., Baker, J.C., and Ames, B.N. (1987) Detection and characterization of lipid hydroperoxides at picomole levels by high-performance liquid chromatography. *Anal. Biochem.* **160**, 7–13
19. Chan, H.W. and Levett, G. (1977) Autoxidation of methyl linoleate. Separation and analysis of isomeric mixtures of methyl linoleate hydroperoxides and methyl hydroxylinoleates. *Lipids* **12**, 99–104
20. Janzen, E.G., Jandrisits, L.T., Shetty, R.V., Haire, D.L., and Hilborn, J.W. (1989) Synthesis and purification of 5, 5-dimethyl-1-pyrroline-*N*-oxide for biological applications. *Chem.-Biol. Interactions* **70**, 167–172
21. Hamer, J. and Macaluso, A. (1964) Nitrones. *Chem. Rev.* **64**, 473–495
22. McCord, J.M. and Fridovich, I. (1969) Superoxide dismutase. An enzymic function for erythrocuprein (hemocuprein). *J. Biol. Chem.* **244**, 6049–6055
23. Buettner, G.R. (1987) Spin trapping: ESR parameters of spin adducts. *Free Radic. Biol. Med.* **3**, 259–303
24. Nakano, M. (1990) Determination of superoxide radical and singlet oxygen based on chemiluminescence of luciferin analogs in *Methods Enzymol* (Packer, L., ed.) Vol.186, pp. 585–591, Academic Press, London and New York
25. Finkelstein, E., Rosen, G.M., and Rauckman, E.J. (1980) Spin trapping. Kinetics of the reaction of superoxide and hydroxyl radicals with nitrones. *J. Amer. Chem. Soc.* **102**, 4994–4999
26. Koga, S., Nakano, M., and Uehara, K. (1991) Mechanism for the generation of superoxide anion and singlet oxygen during heme compound-catalyzed linoleic acid hydroperoxide decomposition. *Arch. Biochem. Biophys.* **289**, 223–229
27. Russell, G.A. (1957) Deuterium-isotope effects in the autoxidation of aralkyl hydrocarbons. Mechanism of the interaction of peroxy radicals. *J. Amer. Chem. Soc.* **79**, 3871–3877
28. Dikalov, S.I. and Mason, R.P. (2001) Spin trapping of polyunsaturated fatty acid-derived peroxyl radicals: Reassignment to alkoxyl radical adducts. *Free Radic. Biol. Med.* **30**, 187–197
29. Akutsu, K., Nakajima, H., Katoh, T., Kino, S., and Fujimori, K. (1995) Chemiluminescence of *Cypridina* luciferin analogues. Part 2. Kinetic studies on the reaction of 2-methyl-6-phenylimidazo [1,2-*a*] pyrazin-3(7*H*)-one (CLA) with superoxide: hydroperoxyl radical is an actual active species used to initiate the reaction. *J. Chem. Soc. Perkin Trans 2*, 1699–1706
30. Ingold, K.U., Paul, T., Young, M.J., and Doiron, L. (1997) Invention of the first azo compound to serve as a superoxide thermal source under physiological conditions: Concept, synthesis, and chemical properties. *J. Amer. Chem. Soc.* **119**, 12364–12365
31. von Sonntag, C. and Schuchmann, H.-P. (1991) The elucidation of peroxyl radical reactions in aqueous solution with the help of radiation-chemical methods. *Angew. Chem. Int. Ed. Engl.* **30**, 1229–1253
32. Stolze, K., Udilova, N., and Nohl, H. (2000) Lipid radicals: Properties and detection by spin trapping. *Acta Biochim. Pol.* **47**, 923–930